Elastic tissue forces mask muscle fiber forces underlying muscle spindle Ia afferent firing rates in stretch of relaxed rat muscle

Kyle P. Blum[1,2], Paul Nardelli[3], Timothy C. Cope[1,3,4], Lena H. Ting[1,4]
[1]Wallace H. Coulter Dept. of Biomedical Engineering, Georgia Institute of Technology, Atlanta, GA 30332
[2*]Dept. of Physiology, Feinberg School of Medicine, Northwestern University, Chicago, IL 60611
[3]School of Biological Sciences, Georgia Institute of Technology, Atlanta, GA 30332
[4]Dept. of Rehabilitation Medicine, Division of Physical Therapy, Emory University, Atlanta, GA 30322

[*]Current address for KPB

Corresponding Author: Lena H. Ting (lting@emory.edu)

Keywords: muscle spindle, proprioception, somatosensation, sensorimotor control

Summary statement: Muscle spindle afferent firing rates are closely related to estimated history-dependent muscle fiber force and yank, suggesting that they signal internal muscle forces and not those of the whole musculotendon.

Abstract

Stretches of relaxed cat and rat muscle elicit similar history-dependent muscle spindle Ia firing rates that resemble history-dependent forces seen in single activated muscle fibers (Nichols and Cope, 2004). Due to thixotropy, whole musculotendon forces and muscle spindle firing rates are history-dependent during stretch of relaxed cat muscle, where both muscle force and muscle spindle firing rates are elevated in the first stretch in a series of stretch-shorten cycles (Blum et al., 2017). By contrast, rat musculotendon exhibits only mild thixotropy such that the measured forces when stretched cannot explain history-dependent muscle spindle firing rates in the same way (Haftel et al., 2004). We hypothesized that history-dependent muscle spindle firing rates elicited in stretch of relaxed rat muscle mirror history-dependent muscle fiber forces, which are masked at the level of whole musculotendon force by extracellular tissue force. We removed estimated extracellular tissue force contributions from recorded musculotendon force using an exponentially-elastic tissue model. We then show that the remaining estimated muscle fiber force resembles history-dependent muscle spindle firing rates recorded simultaneously. These forces also resemble history-dependent forces recorded in stretch of single activated fibers that are attributed to muscle cross-bridge mechanisms (Campbell and Moss, 2000). Our results suggest that history-dependent muscle spindle firing in both rats and cats arise from history-dependent forces due to thixotropy in muscle fibers.

Introduction

Muscle spindles are sensory organs within skeletal muscles that are crucial for sensing body segment position and motion (Prochazka and Ellaway, 2012) with mechanosensory signaling characteristics that generalize across species (Vincent et al., 2017). In relaxed muscle, muscle spindle Ia afferents fire when stretched by an external load, beginning with a high-frequency initial burst, followed by firing related to stretch amplitude and velocity in cats, rats, toads, humans and other species (Banks et al., 1997; Blum et al., 2017; Vincent et al., 2017). These responses are history dependent, such that the first stretch in a series of identical stretch-shorten cycles elicits responses to ramp stretches that are absent or reduced in subsequent stretches (Banks et al., 1997; Blum et al., 2017; Haftel et al., 2004; Matthews, 1972).

In anesthetized cats, history-dependent spindle firing rates mirror history-dependent whole musculotendon forces during muscle stretch due to thixotropy (Campbell and Moss, 2000). In muscles, thixotropy manifests as elevated eccentric force when stretched after the muscle is held at rest versus moving. We previously showed that thixotropy evident in whole cat musculotendon force and yank, i.e. the first time-derivative of force (Lin et al. in review), precisely reproduce the fine temporal details of history dependent firing of Ia afferents in a series of stretch-shorten cycles (Blum et al., 2017).

In anesthetized rats, however, history-dependent muscle spindle firing rates cannot be directly explained by thixotropy, as whole musculotendon forces appear similar in stretch-shorten cycles (Haftel et al., 2004). Rat musculotendon force profiles are qualitatively different than those observed in cat, exhibiting an exponential increase in force during ramp stretches. As longer strains were imposed in prior rat vs. cat studies (7% vs. 3%L_o) increased extracellular matrix (ECM) engagement likely caused the exponential rise in musculotendon force (Gillies and Lieber, 2011).

Here we hypothesized that thixotropy in muscle fibers is masked by ECM forces throughout the muscle when examining whole musculotendon force during muscle stretch in anesthetized rats. We further hypothesized that muscle fiber forces, consisting of both contractile (e.g. actin-myosin forces) and noncontractile components (e.g. titin), in rats exhibit similar history-dependence as muscle spindle Ia firing rates recorded simultaneously. We made the simplifying assumption that ECM and muscle fiber forces act in parallel, contributing additively to musculotendon force. ECM forces were estimated

using a simple exponential-linear tissue model, and muscle fiber force was estimated by analytically removing ECM force from recorded musculotendon force. We found a large proportion of musculotendon force was carried by the estimated ECM. Our data indicate that the muscle fibers are thixotropic, as the estimated muscle fiber force and its first time derivative, yank (Lin et al. in review), were history-dependent and closely resembled history-dependent muscle spindle firing rates recorded simultaneously. Our work suggests that history-dependent spindle firing and muscle fiber forces in rats and cats arise from thixotropy in muscle fibers.

Methods

Animal care

All procedures and experiments were approved by the Georgia Institute of Technology's Institutional Animal Care and Use Committee. Adult female Wistar rats (N=5; 250 - 300 g) were studied in terminal experiments only and were not subject to any other experimental procedures. All animals were housed in clean cages and provided food and water ad libitum in a temperature- and light-controlled environment in Georgia Institute of Technology's Animal Facility.

Terminal physiological experiments

Experiments were designed to measure the firing of individual muscle afferents in response to muscle stretch *in vivo* using electrophysiological techniques as documented previously (Vincent et al., 2017). Rats were deeply anesthetized (complete absence of withdrawal reflex) by inhalation of isoflurane, initially in an induction chamber (5% in 100% O_2) and, for the remainder of the experiment, via a tracheal cannula (1.5–2.5% in 100% O_2).

The triceps-surae muscle group in the left hindlimb was dissected free of surrounding tissue and detached at its insertion together with a piece calcaneus bone. The severed insertion of the left triceps-surae muscle group was securely attached directly to the lever arm of a force and length-sensing servomotor (Model 305B-LR, Aurora Scientific Inc.), to control muscle stretch while recording muscle length and force (dual-mode lever arm system, Aurora Scientific). Initial muscle tension was set to 0.1 N, the approximate passive tension observed for ankle and knee angles of 90° and 120°, respectively.

Triceps surae sensory axons were randomly sampled by intra-axonal penetration in dorsal rootlets and selected for detailed study when identified as group Ia based on several criteria (Vincent et al., 2017). Afferents were identified as low threshold mechanoreceptors supplying triceps surae muscles via electrical stimulation of triceps surae nerves. Group Ia afferents were identified via silencing during electrically-evoked isometric twitch contractions and firing characteristics to stretch and tendon vibration (Vincent et al., 2017).

Firing rates and patterns of Ia afferents were studied in response to length-servo controlled stretches applied to triceps surae muscles at rest. Ramp-release stretches at constant velocity (4 mm/s) were applied with amplitudes ranging from 0.5 to 3 mm. Trials of 3-5 sequences were repeated in between rest periods of at least 10 seconds allowing expression of history dependent firing responses (Fig 1B; (Haftel et al., 2004)). Musculotendon force, length, and Ia-afferent action potentials were simultaneously recorded at a minimum 20kHz and down-sampled to at least 1kHz for analysis. Yank was calculated as the time-derivative of recorded force (Lin et al. 2018, in review).

Muscle fiber force estimation

To isolate the muscle fiber force component, we assumed ECM was mechanically arranged in parallel to muscle fibers (Fig. 1C). We modeled ECM as elastic with both exponential and linear stiffness (Fig. 1D; (Gillies and Lieber, 2011)):

$$F_{nc} = k_{lin}(L - L_0) + Ae^{k_{exp}(L-L_0)}$$

where L is the entire musculotendon length, L_0 is the musculotendon initial length, and k_{lin}, A, and k_{exp} are constants for linear and exponential elements, respectively. ECM forces were subtracted from the recorded force to estimate the muscle fiber force, which resembled muscle spindle IFRs (Fig. 1E). For each muscle (N = 5), k_{lin}, A, and k_{exp} were initialized to values of 0.5 and optimized such that resulting estimated muscle fiber force, when multiplied by a constant, could explain the maximum amount of variance of the recorded Ia afferent IFR during 2mm or 3mm stretch trials (Blum et al., 2017). Parameters from one stretch in each animal was then applied in all other stretches of that muscle.

Variance accounted for of musculotendon force by estimated ECM force

We estimated the contribution of ECM to recorded musculotendon force at each perturbation length for a muscle. We used variance accounted for, defined as:

$$VAF = 100\frac{\sum_t \left(F(t) - F_{fib}(t)\right)^2}{\sum_t F(t)^2}$$

where the numerator represents the sum of squares of the ECM model for a given trial and the denominator is the total sum of squares of the recorded musculotendon force for the same trial.

Estimated driving potential of muscle spindle afferents

To demonstrate that, in principle, arbitrary combinations of estimated muscle fiber force and yank could explain muscle spindle afferent firing rates, we added force and yank together in a pseudolinear manner (Blum et al., 2017):

$$\widehat{IFR} = (F(t) + b_F) * k_F + (Y(t) + b_Y) * k_Y + C$$

k_F and k_Y, respectively, are constant weights on fiber force and yank. b_F and b_Y, respectively, are constant offsets on fiber force and yank. C is a constant. For visualization, we chose these parameters to be k_F = 1393 spikes/Ns, k_Y = 3.6 spikes/N, b_F = 10 N, b_Y = 5N/s, and C = 34 spikes/s. The yank and force components were subjected to a force threshold to emulate the spiking threshold of the neuron.

Statistics

Mean and standard deviation of ECM model parameters k_{lin}, A, and k_{exp} were calculated across animals (N = 5). Mean VAF was calculated for each stretch length across animals to approximate the contribution of ECM forces to the recorded musculotendon force. First, the mean VAF across trials for each stretch length (0.5, 1.0, 2.0, and 3.0 mm) and each animal (N = 5) was calculated (note: trials from at least 3 animals were used for each stretch length except 0.5 mm, for which we only collected data from 1 animal). Then, the mean and standard error of the mean (SEM) of these values was

calculated across animals, resulting in a single mean VAF ± SEM range for each stretch length (4 ranges total).

Results and Discussion

Rat muscle spindle Ia afferents exhibited history-dependent firing rates in response to repeated ramp-release stretches (Haftel et al., 2004). Initial bursts at the onset of the first stretch, and elevated firing rates during the first ramp were observed (Fig 1B). In contrast, simultaneously-recorded musculotendon force did not appear history-dependent, apart from a small rise at stretch onset visible as a brief peak in yank (Fig. 1B). We observed an exponentially increasing force with stretch length (Fig. 1C).

ECM force contributions to whole musculotendon force increased with stretch length (Fig 1D). Both the whole musculotendon force and yank signal exhibited a similar nonlinear rise with applied length: a property of an exponential relationship (Fig 1D). The ECM component was thus modeled by linear and exponential parameters of k_{lin} = 0.0497 ± 0.0388, A = 0.0454 ± 0.317, k_{lin} = 1.071 ± 0.362 (mean ± sd.; N=5 muscles). Using a single set of parameters for each muscle, the estimated ECM component accounted for 53 ± 3% (mean ± SEM) of the total variance in force for 3 mm stretches, 34 ± 3% for 2 mm stretches, 12 ± 1% for 1 mm stretches, and only 3% (data from 1 muscle) for 0.5 mm stretches.

Muscle thixotropy was reflected in the remaining signal representing the force in the muscle fibers and their series elements over time (Fig. 1E). This fiber force had a pronounced initial force rise and larger initial peak in the first stretch (Fig. 1E). This was accompanied by a larger peak in yank (Fig. 1E). Additionally, this rapid force increased resulting in a higher overall level of force during the first ramp stretch compared to subsequent stretches (Fig 1E).

The history-dependence of muscle spindle firing rates, whole musculotendon force and yank, and estimated muscle fiber force and yank are illustrated by differences in the first stretch response versus subsequent responses (Fig. 2A). Muscle spindle firing rates were dramatically different on the first stretch relative to those on subsequent stretches (Fig. 2B, compare yellow to other colored traces).

However, total musculotendon force and yank were quite similar across all stretches with only small differences between the first and subsequent stretches (Fig. 2C). Similarly, the estimated muscle fiber force and yank were clearly differentiated on the first ramp-release stretch (Figure 2D). However, neither muscle fiber force nor yank individually resembled the history dependence of the spindle firing rates.

History dependence seen in muscle spindle firing rates (Fig. 3A, B) resembled linear combinations of muscle fiber force and yank, subject to a threshold (Fig. 3C, D). Although muscle spindle firing rates in 0.5 mm stretches (e.g. Fig 3B) were qualitatively different than 2 mm stretches (Fig 3A), they were still similar to the linear combinations of the estimated muscle fiber force and yank (Fig. C, D). These estimates were generated using the same weighting of force and yank at both stretch lengths (Fig. 3 E, F). This robustness is all the more remarkable because the same ECM properties were used to estimate muscle fiber force and yank (Fig 3 G, H) at different stretch lengths where the amplitude of the ECM forces differed dramatically (30.2% vs 3.1% VAF of the total musculotendon force, respectively). In particular the flatter muscle spindle response during the first ramp-release (Fig. B, yellow trace) was also present in the linear combination of muscle fiber force and yank (Fig. 3D, yellow trace).

In summary, history-dependent muscle fiber forces during stretch of relaxed rat muscle can be identified from whole musculotendon force even when the majority of that force arises from stretch of ECM. ECM force dominated the musculotendon force and yank traces, consistent with reports that muscle fibers carry as little as 15% of total musculotendon loads in rodents (Meyer and Lieber, 2011; Meyer and Lieber, 2018). The remaining residual force was a relatively small component of the total force but resembled characteristics of isolated, activated, muscle fibers in ramp-release stretches (Campbell and Lakie, 1998; Campbell and Moss, 2000; Campbell and Moss, 2002), with an initial short-range stiffness (Getz et al., 1998), as well as higher mean force during the first ramp stretch.

The estimated muscle fiber forces exhibited thixotropic characteristics that were similar to history-dependence in muscle spindle afferents recorded simultaneously, suggesting similar muscle force mechanisms in both cats and rats. The thixotropy we studied has been suggested to arise from muscle-cross bridge attachments and only occurs in the presence of Ca++ (Campbell and Moss, 2002),

although activation-dependent titin stiffness has also been suggested as a potential mechanism (Labeit et al., 2003). It appears that these well-known thixotropic properties of muscle fibers dominate history-dependence in musculotendon force, and considering thixotropic properties of ECM (Barbenel et al., 1973) would not qualitatively alter our interpretations. The firing rate of muscle spindle primary afferents is directly related to the intrafusal muscle fibers of the spindle, with only a small amount of connective tissue force contributing to spike-generation (Banks et al., 1997; Boyd et al., 1977). In relaxed muscle we assume that the intrafusal and extrafusal muscle force exhibit similar responses to stretch; thus, we used the estimate of muscle fiber force as a proxy for intrafusal force. Our work shows that history-dependence in both rat and cat muscle spindles arises from thixotropic effects on muscle fiber force when stretched. While the result demonstrated in this paper supports our hypothesis, more comprehensive studies should be performed to more quantitatively describe this mechanism.

Our study further provides a neuromuscular explanation for the tendency of human subjects to underestimate forces at longer musculotendon lengths due to the stretch of ECM. Psychophysical studies demonstrate that human participants tend to only perceive forces generated by muscle fibers, and not passive components of force (Tsay et al., 2014). This sense of "fiber-only" force is consistent with the finding in the present study that muscle spindles only fire in response to the force in muscle fibers, but not in ECM. While Golgi tendon organs also sense active muscle force, they are located in-series with both muscle fibers and ECM and are unable to differentiate contractile and non-contractile force. The high contribution of non-contractile forces to whole musculotendon force during muscle stretch in rats could also explain the fact that Golgi tendon organ Ib afferents fire robustly to stretch in rats, but not cats (Vincent et al., 2017).

Taken together, our work suggests muscle spindle firing rate reflect muscle fiber forces during passive stretch across different species. The dissociation of the encoding of muscle fiber and ECM forces may be important in understanding the role of proprioceptors in sensorimotor control, and the similarities and differences across species (Vincent et al., 2017). Differences in prior experiments between cats and rats may simply be due to difference in the relative amplitude of stretches, as larger stretches in cat muscle do engage ECM, which has an exponential characteristic (Gillies and Lieber, 2011; Matthews, 1933) and would likely need to be considered for larger stretch amplitudes. Indeed,

when homologous muscles in the cat, rat, and mouse are stretched with similar strain, firing responses of Ia afferents in each species are similar despite differences in the shape of musculotendon force (Carrasco et al., 2017). Further, in our anesthetized conditions, intrafusal forces within the muscle spindle encoding region is assumed to be similar to the extrafusal muscle force; we speculate that this assumption would also hold when a muscle and spindle are under beta control or alpha-gamma coactivation (Edin and Vallbo, 1990; Prochazka and Gorassini, 1998), but not when gamma motor drive differs significantly from alpha motor drive. We hypothesize the fundamental idea that muscle spindles fire in response to intrafusal muscle force and yank generalizes across both passive and active movement conditions, reinforcing the necessity of considering intrafusal muscle state when examining muscle spindle function.

Funding

This work was supported by the National Institutes of Health [R01 HD90642 to L.H.T. and T.C.C., P01 NS057228 to T.C.C., F31 NS093855 to K.P.B.].

References Cited

Banks, R. W., Hulliger, M., Scheepstra, K. A. and Otten, E. (1997). Pacemaker activity in a sensory ending with multiple encoding sites: the cat muscle spindle primary ending. *J. Physiol. (Lond.)* **498 (Pt 1)**, 177–199.

Blum, K. P., Lamotte D'Incamps, B., Zytnicki, D. and Ting, L. H. (2017). Force encoding in muscle spindles during stretch of passive muscle. *PLoS Comput Biol* **13**, e1005767–24.

Boyd, I. A., Gladden, M. H., McWilliam, P. N. and Ward, J. (1977). Control of dynamic and static nuclear bag fibres and nuclearbag fibres and nuclear chain fibres by gamma and beta axons in isolated cat muscle spindles. *J. Physiol. (Lond.)*.

Campbell, K. S. and Lakie, M. (1998). A cross-bridge mechanism can explain the thixotropic short-range elastic component of relaxed frog skeletal muscle. *J. Physiol. (Lond.)* **510 (Pt 3)**, 941–962.

Campbell, K. S. and Moss, R. L. (2000). A thixotropic effect in contracting rabbit psoas muscle: prior movement reduces the initial tension response to stretch. *J. Physiol. (Lond.)*.

Campbell, K. S. and Moss, R. L. (2002). History-Dependent Mechanical Properties of Permeabilized Rat Soleus Muscle Fibers. *Biophysical Journal* **82**, 929–943.

Carrasco, D. I., Vincent, J. A. and Cope, T. C. (2017). Distribution of TTX-sensitive voltage-gated sodium channels in primary sensory endings of mammalian muscle spindles. *Journal of Neurophysiology* **117**, 1690–1701.

Edin, B. B. and Vallbo, A. B. (1990). Muscle afferent responses to isometric contractions and relaxations in humans. *Journal of Neurophysiology* **63**, 1307–1313.

Getz, E. B., Cooke, R. and Lehman, S. L. (1998). Phase Transition in Force during Ramp Stretches of Skeletal Muscle. *Biophysical Journal* **75**, 2971–2983.

Gillies, A. R. and Lieber, R. L. (2011). Structure and function of the skeletal muscle extracellular matrix. *Muscle & nerve*, ***44*(3)**, 318-331.

Haftel, V. K., Bichler, E. K., Nichols, T. R., Pinter, M. J. and Cope, T. C. (2004). Movement Reduces the Dynamic Response of Muscle Spindle Afferents and Motoneuron Synaptic Potentials in Rat. *Journal of Neurophysiology* **91**, 2164–2171.

Labeit, D., Watanabe, K., Witt, C., Fujita, H., Wu, Y., Lahmers, S., Funck, T., Labeit, S. and Granzier, H. (2003). Calcium-dependent molecular spring elements in the giant protein titin. *PNAS* **100**, 13716–13721.

Lin, D. C., McGowan, C. P., Blum, K. P. and Ting, L. H. Yank: the time derivative of force is an important biomechanical variable in sensorimotor systems. *Journal of Experimental Biology*.

Matthews, B. H. C. (1933). Nerve endings in mammalian muscle. *The Journal of Physiology* **78**, 1–53.

Matthews, P. B. C. (1972). Mammalian muscle receptors and their central actions. Baltimore, MD, USA: Williams & Wilkins.

Meyer, G. A. and Lieber, R. L. (2011). Elucidation of extracellular matrix mechanics from muscle fibers and fiber bundles. *J Biomech* **44**, 771–773.

Meyer, G. and Lieber, R. L. (2018). Muscle fibers bear a larger fraction of passive muscle tension in frogs compared with mice. *Journal of Experimental Biology* **221**, jeb182089–5.

Nichols, T. R. and Cope, T. C. (2004). Cross-bridge mechanisms underlying the history-dependent properties of muscle spindles and stretch reflexes. *Can. J. Physiol. Pharmacol.* **82**, 569–576.

Prochazka, A. and Ellaway, P. (2012). *Sensory Systems in the Control of Movement*. Hoboken, NJ, USA: John Wiley & Sons, Inc.

Prochazka, A. and Gorassini, M. (1998). Ensemble firing of muscle afferents recorded during normal locomotion in cats. *The Journal of Physiology* **507**, 293–304.

Tsay, A., Savage, G., Allen, T. J. and Proske, U. (2014). Limb position sense, proprioceptive drift and muscle thixotropy at the human elbow joint. *The Journal of Physiology* **592**, 2679–2694.

Vincent, J. A., Gabriel, H. M., Deardorff, A. S., Nardelli, P., Fyffe, R. E. W., Burkholder, T. and Cope, T. C. (2017). Muscle proprioceptors in adult rat: mechanosensory signaling and synapse distribution in spinal cord. *Journal of Neurophysiology* **118**, 2687–2701.

Figures

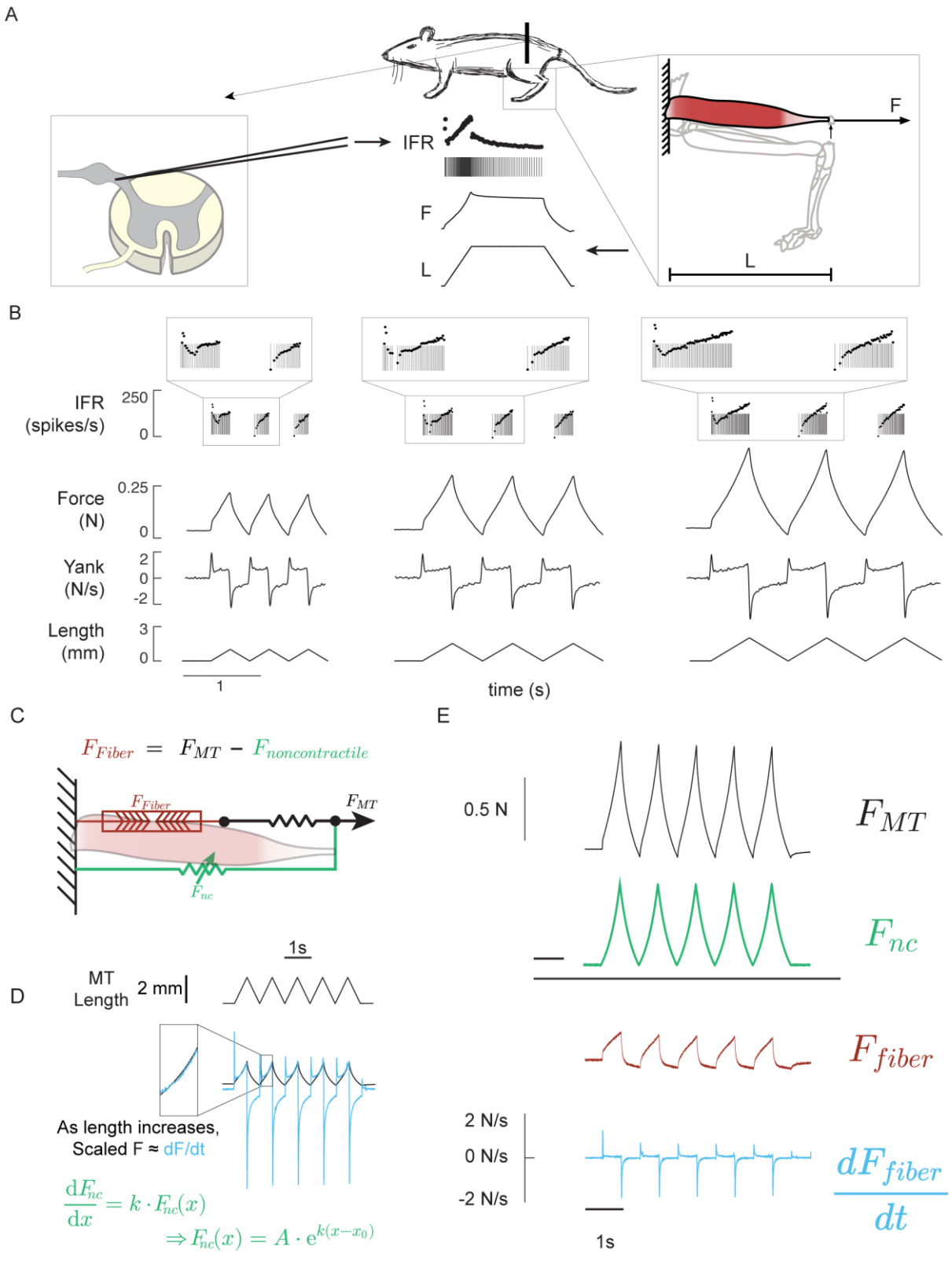

Figure 1: Methods for recording muscle spindle firing rates and estimating muscle fiber force during stretch of relaxed rat muscle. A) Intra-axonal recording from muscle spindle Ia afferents from in dorsal rootlet were recorded during stretch of the triceps surae musculotendon. Muscle length (L) and total musculotendon force (F; panel on right) were recorded with membrane potentials; instantaneous firing rate were computed based on action potential events (IFR; traces in center panel). B) Sets of identical triangular stretches were imposed at three lengths (1 mm, 2 mm, and 3mm). Action potentials (gray lines) with superimposed instantaneous firing rate (black dots) are shown temporally aligned with simultaneously recorded muscle force, yank and length traces. In each trial, muscle spindle Ia firing response to identical stretch stimuli different in the first stretch when compared with subsequent stretches. Specifically, the response to the first stretch contains an initial burst of spikes at stretch onset and more pronounced dynamic response post-initial burst. C) The recorded musculotendon force was assumed to be comprised two additive force components: one component arising from noncontractile tissues (green) with an elastic force-length relationship and another component arising from the muscle fibers (red) and series elastic component (black). D) Musculotendon force (black) and yank (cyan) are overlaid to show similar exponential rise with imposed stretch (above). This suggests a large component of the recorded musculotendon force arises due to an exponential elastic force. E) Subtracting the estimated noncontractile force component (green) from the recorded musculotendon force (black) yielded the estimated muscle fiber force (red) and yank (blue), both of which were history dependent, with a larger response during the first stretch.

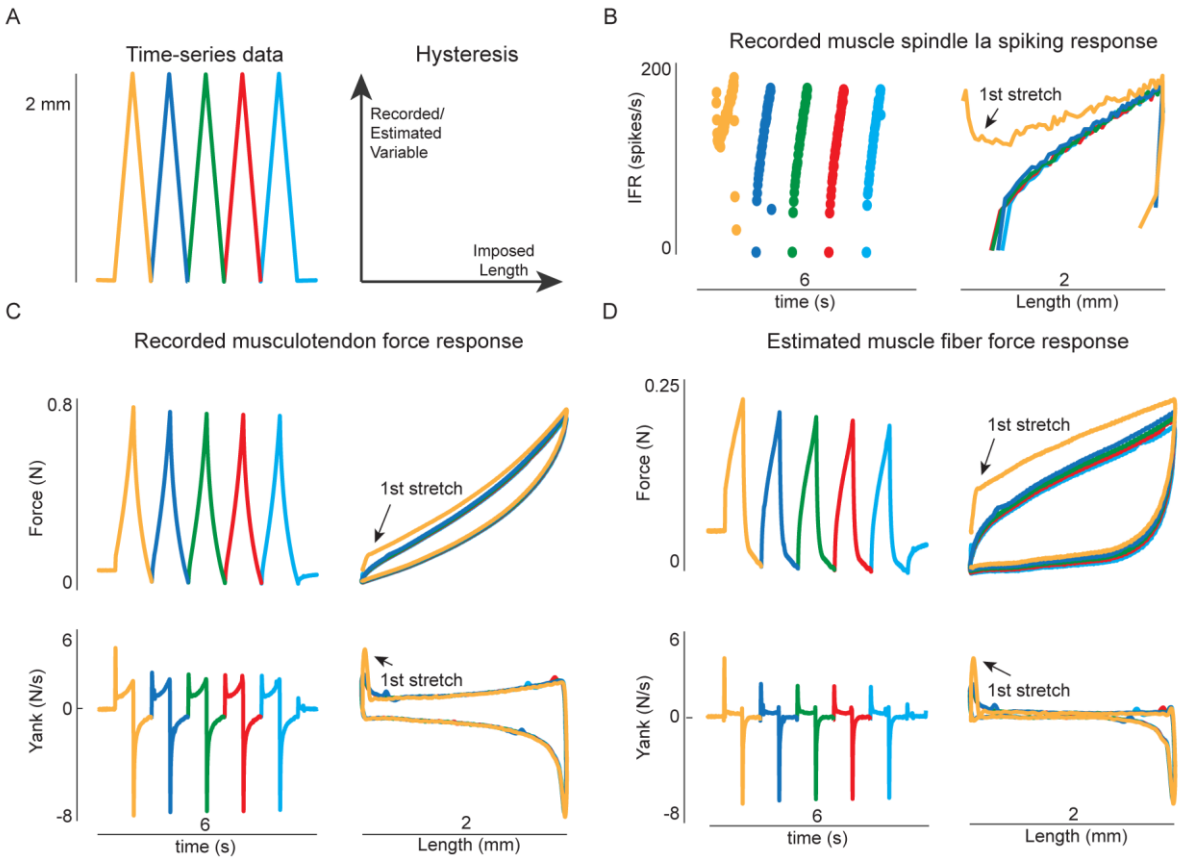

Figure 2: History-dependence of muscle spindle firing rates, musculotendon force and yank, and muscle fiber force and yank. A) Applied length depicted as time series (left panel). Different colors represent different stages of the perturbation. B) Recorded firing rate from Ia afferent to applied length from A. Represented as time series (left) and as a function of length (right). C) Recorded musculotendon force (top) and yank (bottom) D) Estimated muscle fiber force (top) and yank (bottom) estimated from musculotendon force in C.

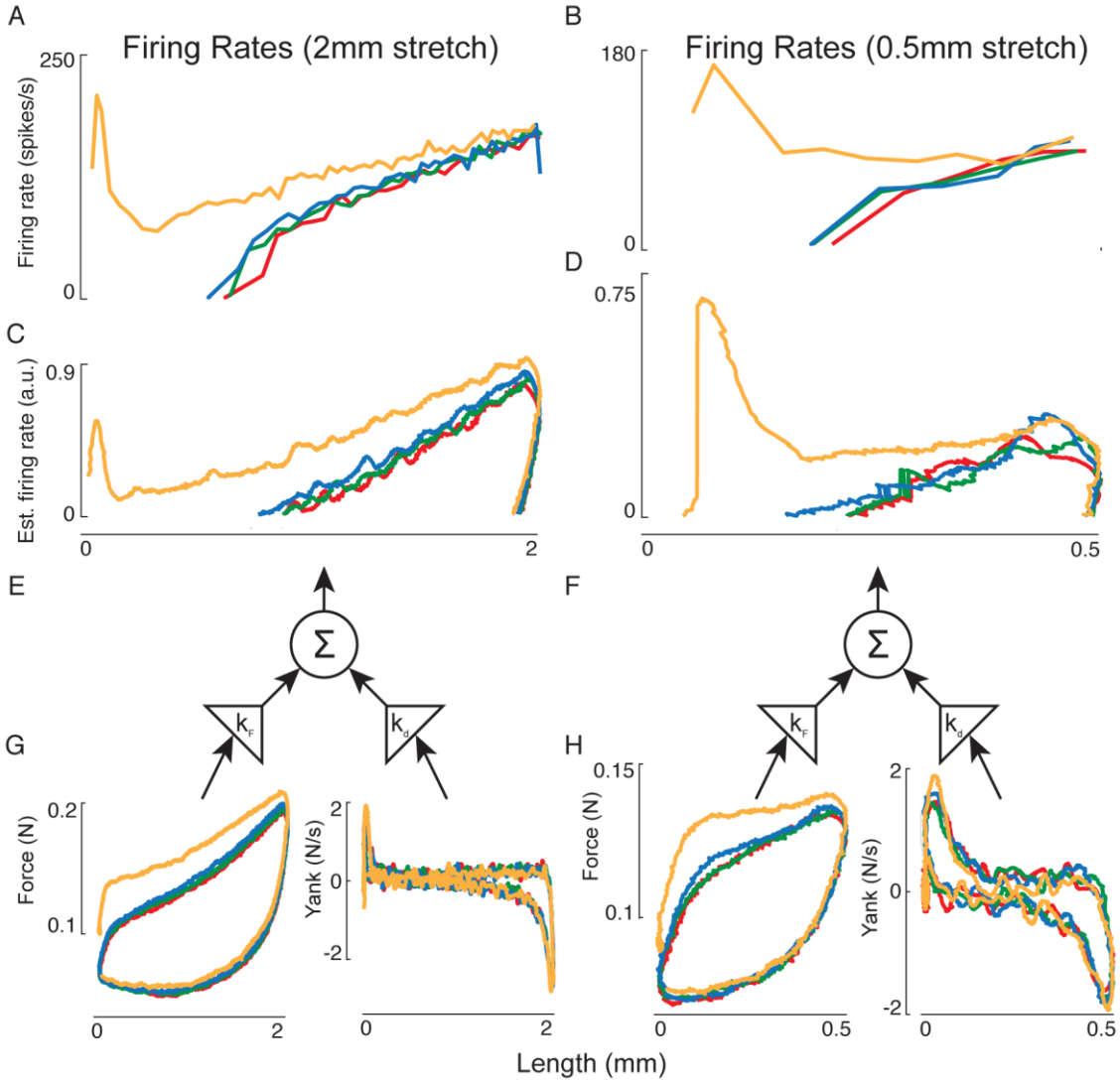

Figure 3: History-dependent muscle spindle firing rates at different applied lengths resembled linear combinations of muscle fiber force and yank subject to a threshold. Muscle spindle firing rate for the afferent in A) 2 mm and B) 0.5 mm stretches. C, D) Linear combination of estimated muscle fiber force and yank subject to a threshold exhibited the same qualitative features in both stretch conditions (a.u. – arbitrary units). E, F) The same weights (and offsets, not shown in diagram) were used in both stretch amplitudes to combine G, H) estimated muscle fiber force and yank signals.